and in approaches leading to production of virus-free sugarcane planting material by tissue-culture technology.

1. Agnihothri, V. P., Current sugarcane scenario and management strategies. *Indian Phytopathol.*, 1996, **49**, 109–126.
2. Jain, R. K., Rao, G. P. and Varma, A., Present status of management of sugarcane mosaic virus. In *Plant Virus Disease Control* (eds Hadidi, A., Khetarpal, R. K. and Koganezava, H.), APS Press, St Paul, Minnesota, USA, 1998, pp. 495–523.
3. Hall, J. S., Adams, B., Parsons, T. J., French, R., Lane, L. C. and Jenson, S. G., Molecular cloning, sequencing and phylogenetic relationships of a new potyvirus sugarcane streak mosaic virus and a re-evaluation of the classification of the Potyviridae. *Mol. Phylogenet. Evol.*, 1998, **10**, 323–332.
4. Hema, M., Joseph, J., Gopinath, K., Sreenivasulu, P. and Savithri, H. S., Molecular characterization and interviral relationships of a flexuous filamentous virus causing mosaic disease of sugarcane (*Saccharum officinarum* L.) in India. *Arch. Virol.*, 1999, **144**, 479–490.
5. Rabenstein, F., Seifers, D. L., Schubert, J., French, R. and Stenger, D. C., Phylogenetic relationships, strain diversity and biogeography of tritimoviruses. *J. Gen. Virol.*, 2002, **83**, 895–906.
6. Hema, M., Sreenivasulu, P. and Savithri, H. S., Taxonomic position of sugarcane streak mosaic virus in the family Potyviridae. *Arch. Virol.*, 2002, **147**, 1997–2007.
7. Hema, M., Venkatramana, M., Savithri, H. S. and Sreenivasulu, P., Biological, antigenic and genomic relationships among the virus isolates causing mosaic disease of sugarcane in South India. *Curr. Sci.*, 1999, **77**, 698–702.
8. Hema, M., Savithri, H. S. and Sreenivasulu, P., Antibody and nucleic acid probe based techniques for detection of sugarcane streak mosaic virus causing mosaic disease of sugarcane in India. *Curr. Sci.*, 2001, **81**, 1105–1108.
9. Hema, M., Kirthi, N., Sreenivasulu, P. and Savithri, H. S., Development of recombinant coat protein antibody based IC–RT–PCR for detection and discrimination of sugarcane streak mosaic virus isolates from South India. *Arch. Virol.*, 2003, **148**, 1185–1193.
10. Hema, M., Savithri, H. S. and Sreenivasulu, P., Sugarcane streak mosaic virus: Occurrence, purification, characterization and detection. In *Sugarcane Pathology: Virus and Phytoplasma Diseases* (eds Rao, G. P. *et al.*), Science Publishers, Inc., USA, 2001, vol. 2, pp. 37–70.
11. Berger, P. H., Thornbury, D. W. and Pirone, T. P., Detection of picogram quantities of potyviruses using dot-blot immunobinding assay. *J. Virol. Methods*, 1985, **12**, 31–36.
12. Nalasco, G., de Blas, C., Torres, V. and Ponz, F., A method combing immunocapture and PCR amplification in a microtiter plate for the detection of plant viruses and sub-viral pathogens. *J. Virol. Methods*, 1999, **45**, 201–218.
13. Sambrook, J., Fritsch, E. F. and Maniatis, T., *Molecular Cloning – A Laboratory Manual*, Cold Spring Harbor, New York, 1989, vol. 3.
14. Rowhani, A., Maningas, M. A., Lile, L. S., Daubert, S. and Golino, D. A., Development of a detection system for viruses of woody plants based on PCR analysis of immobilized virions. *Phytopathology*, 1995, **85**, 347–352.

ACKNOWLEDGEMENTS. M.H. is a recipient of Research Associateship from the Council of Scientific and Industrial Research, New Delhi. We thank Prof. V. Muniyappa, University of Agricultural Sciences, Bangalore for providing healthy sugarcane.

Received 25 July 2003; revised accepted 18 September 2003

Leaf area index retrieval using IRS LISS-III sensor data and validation of MODIS LAI product over Madhya Pradesh

M. R. Pandya[†,*], K. N. Chaudhari , R. P. Singh[†], V. K. Sehgal[†,#], G. D. Bairagi[‡], R. Sharma[‡] and V. K. Dadhwal

[†]Remote Sensing Applications and Image Processing Area, Space Applications Centre (Indian Space Research Organization), Ahmedabad 380 015, India
[‡]M P Remote Sensing Applications Centre, MPCOST, Bhopal, India
[#]Present address: Department of Agricultural Physics, Indian Agricultural Research Institute, New Delhi 110 012, India

Results of a study aimed at relating field measurements of leaf area index (LAI) to space-borne IRS LISS-III data, preparation of site-level LAI maps and validation of moderate resolution imaging spectroradiometer (MODIS)-based 1 km LAI global fields, conducted over agricultural areas of Bhopal and Indore during winter season of 2001–02 are presented. Measurements of field-level LAI, aerosol optical thickness and water vapour were carried out on the day of satellite overpass for three dates for each site. Empirical models based on site-specific LAI–vegetation index relations were developed and used to generate 23 m resolution LAI maps. These LAI images covering approximately 30 km × 30 km were aggregated to 1 km spatial resolution and used for validation of MODIS LAI product. The results indicated significant positive correlation between LAI derived from LISS-III data and MODIS data, with an overestimation in the MODIS product, root mean square error of 0.92 to 1.26 for the Bhopal site and 0.20 to 0.33 for the Indore site.

LEAF area index (LAI) is a dimensionless index used to quantify the single-sided vegetation leaf area per unit of ground area. LAI and the fraction of absorbed, photosynthetically-active radiation (FAPAR) (0.4–0.7 μm) strongly control water, carbon and energy exchanges between vegetation and the atmosphere[1]. LAI is a key parameter in productivity models at landscape to global scales[2]. It is an important input for global models of hydrology, biogeochemistry, ecology[3], and land-surface component of general circulation models[4]. LAI, together with other biophysical variables, plays an important role in measurement and monitoring of land surface characteristics that can potentially predict large-scale changes in environment[5]. For effective use in such large-scale models, regional and global LAI must be available over a period of time. Ground measurements of LAI are cumbersome, time-consuming and impossible to obtain at global scale, while

*For correspondence. (e-mail: m_r_pandya@yahoo.com)

satellite remote sensing is the most effective means of estimating LAI global fields on a regular basis.

Recent advanced sensors such as MODIS (moderate resolution imaging spectroradiometer) on-board Earth Observing System (EOS) Terra/Aqua platforms, now provide LAI as a standard product (MOD15) to the scientific community at 1 km resolution, every eight days. The validation of LAI global fields, i.e. assessment of uncertainty of remote sensing-derived products by analytical comparison to reference data which are presumed to represent the target values[6] is necessary and has been carried out for many sites over USA, Africa[7] and elsewhere, but no results are available over India. A LAI retrieval and validation experiment (LRVE) aimed at development of remote sensing-based, site-specific vegetation index–LAI relations and validation of MODIS LAI product was conducted at Indore and Bhopal during the wheat-growing season of 2001–02. The experiment had three components: (i) the field measurements of LAI and atmospheric properties (aerosol optical depth and water vapour); (ii) generation of fine resolution (23 m) LAI maps from IRS LISS-III and field data; and (iii) generation of 1 km LAI maps and their comparison with MODIS LAI product.

Indore lies in the semi-arid and Bhopal lies in the sub-humid zone, and they have black cotton soil. The sites have wheat as a major crop, with a small proportion of the cropped area under gram and pea. The study area and remote sensing data used in the LRVE are shown in Table 1.

Field measurements of LAI were made within a day of satellite acquisition and atmospheric measurements on the day of satellite overpass. LAI was measured in a total of 75 fields (with four measurements per field) using LAI-2000 Plant Canopy Analyzer (LI-COR, USA), which is based on 'fish-eye' measurement of diffuse radiation interception by measuring gap fraction at five zenith angles (approximately 0–13°, 16–28°, 32–43°, 47–58°, 61–74°) simultaneously. The measured gap-fraction data are inverted to obtain the effective LAI. The locations of fields were marked on false colour composite (FCC) paper prints and also determined with global positioning system (GPS), to accurately identify the locations. The aerosol optical thickness (AOT) and water vapour content were measured on the day of IRS-1D satellite acquisitions using hand-held Microtops-II Sunphotometer (Solar light Inc, Philadelphia, USA), which has five optical collimators working at 500, 675, 870, 936 and 1020 nm and a full field-of-view of 2.5°.

Information on sites, date of LAI measurements, crops covered, range of LAI, AOT and water vapour are summarized in Table 2. The range of LAIs across all sites/seasons was from 0.14 to 5.6. The range of AOT measurements collected at the time of satellite pass across the observation dates and sites was 0.16 to 0.32 at 500 nm, and the range of water vapour was 0.71 to 1.28 cm.

A number of techniques ranging from regression models to inversion of canopy reflectance models[8–11] have been adopted for mapping LAI using remote-sensing

Table 1. LAI sites and date of satellite acquisition

		IRS-1D LISS-III*		MODIS LAI product	
Site	Central location longitude, latitude	Date of IRS-1D acquisition	Satellite path/row	Date of eight-day composite product	Tile number
Indore	75°57′E, 22°53′N	2 December 2001	96/56	3–10 December 2001	24H 6V
		27 December 2001		27 December 2001–3 January 2002	
		21 January 2002#		–	
Bhopal	77°28′E, 23°10′N	24 December 2001	97/57	19–26 December 2001	25H 6V
		18 January 2002#		–	
		12 February 2002		10–17 February 2002	

#Overcast conditions, hence not used in analysis.
*LISS-III has green, red, near infrared bands (spatial resolution 23 m), swir band (spatial resolution 70 m).

Table 2. Range of LAI and atmospheric parameters across sites/dates

Site	Date of ground observation	Crop	LAI range	AOT at 500 nm	Water vapour (cm)
Indore	2 December 2001	Wheat, gram	0.17–3.30	0.16	0.71
	27 December 2001	Wheat, gram	0.69–4.63	0.26	1.15
	21 January 2002*	Wheat, gram	0.64–3.26	–	–
Bhopal	24 December 2001	Wheat, gram, pea	0.14–3.80	0.2	0.51
	18 January 2002*	Wheat, gram, pea	1.05–5.6	–	–
	12 February 2002	Wheat, gram, pea	1.25–4.48	0.32	1.28

*Overcast conditions, hence atmospheric measurements were not obtained.

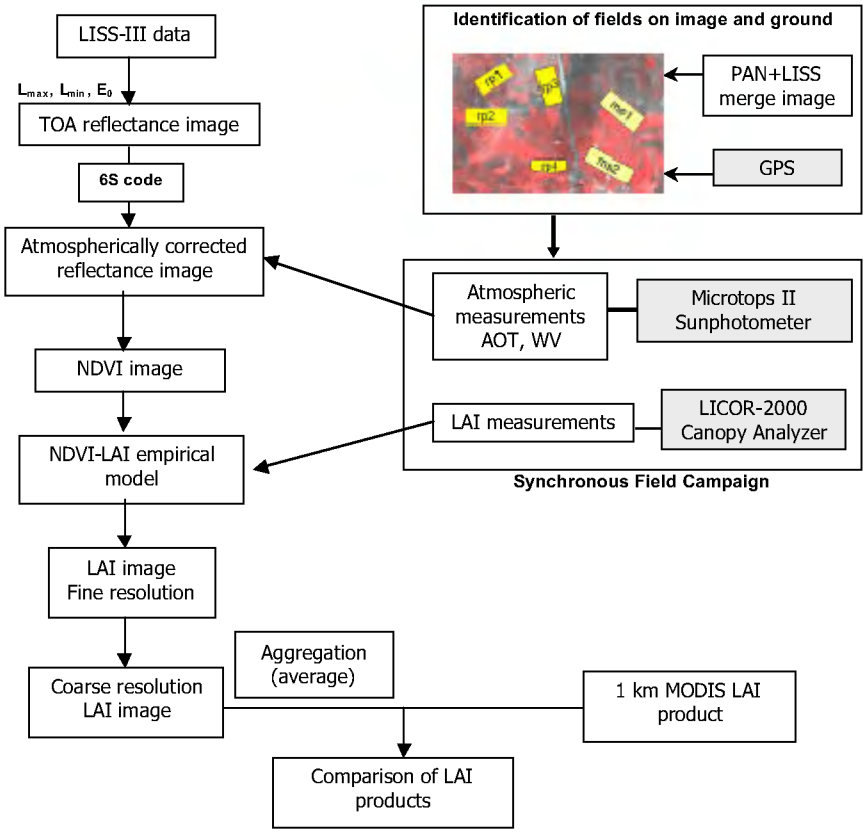

Figure 1. Procedure describing retrieval of LAI from IRS LISS-III data and its comparison with MODIS LAI product.

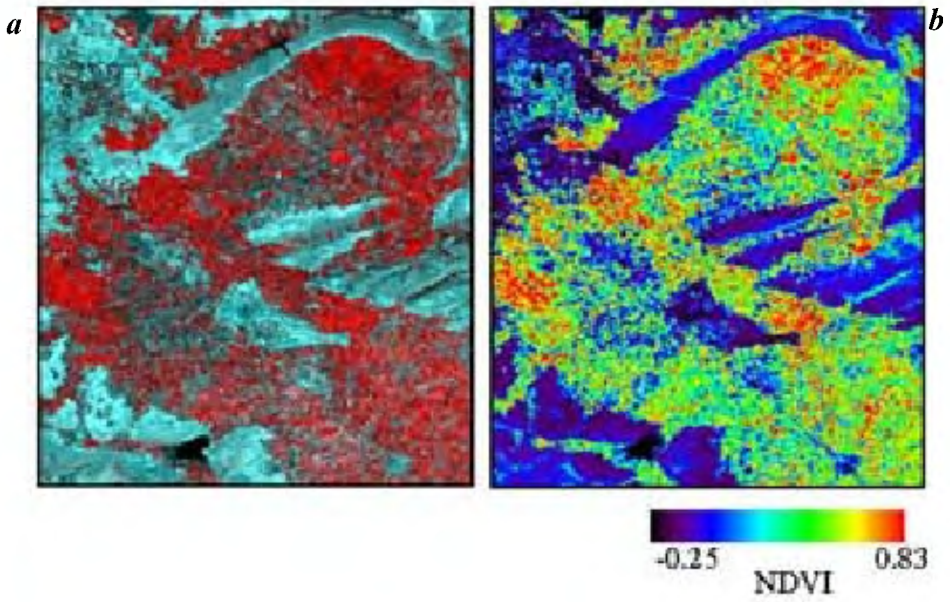

Figure 2. ***a***, False colour composite of Bhopal site (IRS-1D LISS-III, 12 February 2002). ***b***, NDVI image of Bhopal site (12 February 2002).

data. The empirical approach based on NDVI (normalized difference vegetation index = NIR-R/NIR + R) and an exponential model were used to relate remote-sensing observation to field LAI in the present study. The complete procedure is shown in Figure 1. The sub-images over test sites were extracted (Figure 2 *a*) from LISS-III

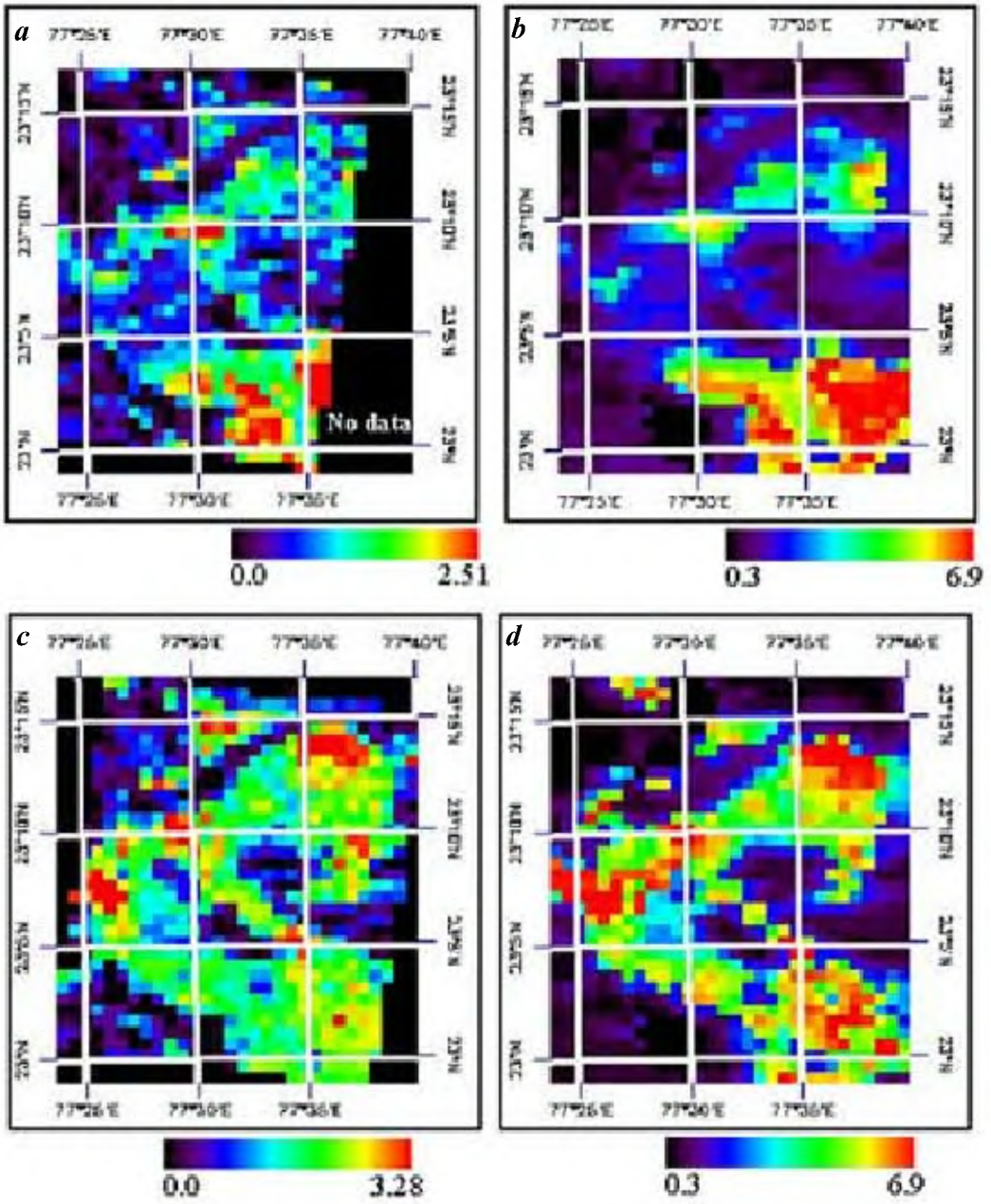

Figure 3. ***a***, LAI map retrieved from LISS-III Bhopal site (24 December 2001). ***b***, MODIS LAI product, eight-day composite (19–26 December 2001). ***c***, LAI map retrieved from LISS-III Bhopal site (12 February 2002). ***d***, MODIS LAI product, eight-day composite (10–17 February 2002).

Table 3. Regression models to relate MODIS LAI and LAI derived from LISS-III data

Site	Date	*a**	*b**	R^2	Root mean square error
Bhopal	24 December 2001	0.433 (0.054)	2.4980 (0.073)	0.61	0.92
	12 February 2002	0.419 (0.089)	1.9874 (0.058)	0.61	1.26
Indore	2 December 2001	0.571 (0.013)	1.1643 (0.04)	0.52	0.20
	27 December 2001	0.681 (0.021)	0.7477 (0.026)	0.51	0.33

Equation: $y = a + bx$, y = MODIS LAI, x = LISS-III LAI.
*Numbers in brackets show root mean square error of individual coefficients.

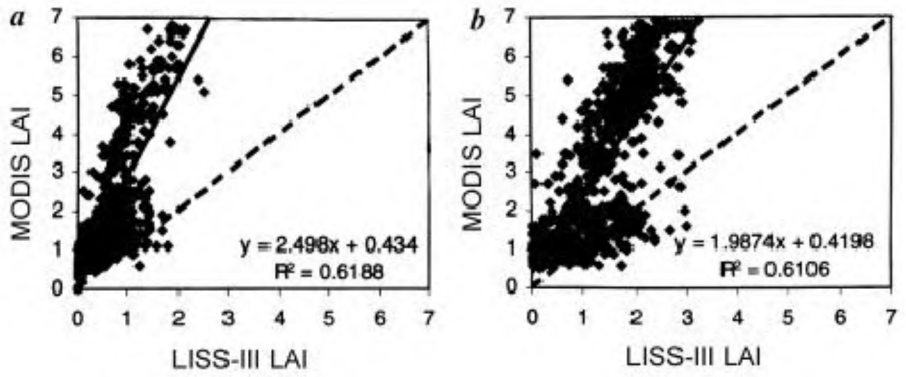

Figure 4. Comparison of LISS-III LAI and MODIS LAI over Bhopal site (*a*) 24 December 2001 and (*b*) 12 February 2002.

data. Digital numbers (DN) were converted to top-of-atmosphere (TOA) reflectance using the sensor gain, offset, sun-angle and exo-atmospheric band-pass coefficients[12]. Surface reflectance was calculated from TOA reflectance using the 6S-code[13], with the atmospheric parameters measured at sites as input. Out of six IRS-1D LISS-III acquisitions (Table 1), two were cloudy and not used in the analysis. The reflectance images were registered to corresponding geo-rectified images using nearest-neighbour resampling, with less than 0.5 pixel root mean square error (rmse). The fields with LAI measurements were identified and demarcated carefully on the corresponding LISS-III and panchromatic (PAN) merged (5.8 m spatial resolution) data. The mean NDVI was computed (Figure 2 *b*) for each field. Three empirical relations, namely linear, exponential and polynomial were examined for the NDVI–LAI relation. Site-specific, non-linear NDVI–LAI relations were developed for each site and acquisition. The exponential and polynomial fits were found to have higher R^2 (0.58–0.73) than the linear fits (0.3–0.52). The exponential form of models was used to generate the fine-resolution LAI maps from LISS-III data for each site and date. These LAI images were aggregated (Figure 3 *a* and *c*) to 1 km spatial resolution using averaging for comparison with MODIS LAI product.

The MODIS LAI products of 1 km spatial resolution and composited over an eight-day period corresponding to $10° \times 10°$ tiles in HDF EOS format were acquired for the study area (Table 1) and reprojected from original integerized sinusoidal projection to UTM projection. The LAI images (Figure 3 *b* and *d*) were generated by applying a scaling factor after masking out water and urban pixels. Quality flags supplied with MODIS LAI products were studied and inter-comparison between LISS-III LAI and MODIS LAI was restricted to pixels pertaining to the class of overall best quality (cloud-free pixels and LAI retrieval through RT model). A preliminary analysis using all pixels, including partially cloudy pixels and LAI retrieval through back-up algorithm, indicated a much higher scatter between MODIS LAI and LISS-III-estimated LAI.

Comparison between LISS-III-derived LAI and MODIS LAI was carried out by performing regression between LAI estimated from MODIS (dependent) and LISS-III (independent) and the results for both sites are summarized in Table 3. Comparison over both sites indicated significant positive correlation between LISS-III-derived LAI and MODIS LAI ($r = 0.78$ for Bhopal and $r = 0.72$ for Indore). A slope of 1 and 0 intercept indicates full match, while deviations show over/under estimation. The analyses indicated an overestimation in MODIS LAI compared to LISS-III LAI for both sites. The scale of overestimation is quite high for Bhopal (slope: 1.98 and 2.49) than Indore (slope: 0.74 and 1.16). Overestimation by LAI was higher for higher LAI estimates by LISS-III, especially in Bhopal (Figure 4). The overall rmse of MODIS LAI is higher for Bhopal (0.92 and 1.26) compared to Indore (0.20 and 0.33); however Bhopal had a higher range of LAI (0.1 to 3.28 in LISS-III LAI, 0.3 to 6.9 in MODIS LAI). A simple two-stream model of Price[14] has also given similar rmse[15]. During the analysis, many pixels of MODIS LAI product were observed to have high LAI (5–6.9), which seems to be unrealistic and contrary to the ground observations. A similar trend was observed for other dates and sites. Since comparison is restricted to only the best RT-model derived pixels, the errors could be due to wrong biome type, vegetation-dependent parameters and effect of soil background or aggregation procedure. Detailed modelling and observation experiments using reflectance data at two different spatial resolutions may be necessary to identify the cause of this overestimation. However, it may be pointed out that LAI is a spatially heterogeneous quantity, and is associated with high uncertainty in field observations and other procedures. Additional studies covering more sites and vegetation types are underway before bringing the MODIS LAI product to operational use.

1. Running, S., Peterson, D., Spanner, M. and Teuber, K., Remote sensing of coniferous forest leaf area. *Ecology*, 1986, **67**, 273–276.
2. Turner, D. P., Cohen, W. B., Kennedy, R. E., Fassnacht, K. S. and Briggs, J. M., Relationships between leaf area index, fapar, and net primary production of terrestrial ecosystems. *Remote Sensing Environ.*, 1999, **70**, 52–68.
3. Sellers, P. J. *et al.*, Modeling the exchange of energy, water and carbon between continents and atmosphere. *Science*, 1997, **275**, 502–509.
4. Buermann, W., Dong, J., Zeng, X., Myneni, R. B. and Dickinson, R. E., Evaluation of the utility of satellite-based vegetation leaf area index data for climate simulations. *J. Climate*, 2001, **14**, 3536–3550.
5. Cohen, W. B. and Justice, C. O., Validating MODIS terrestrial ecology products: linking *in situ* and satellite measurements. *Remote Sensing Environ.*, 1999, **70**, 1–3.
6. Justice, C., Belward, A., Morisette, J., Lewis, P., Privette, J. and Baret, F., Developments in the 'validation' of satellite sensor products for the study of the land surface. *Int. J. Remote Sensing*, 2000, **21**, 3383–3390.
7. Privette, J. L., *et al.*, Early spatial and temporal validation of MODIS LAI product in the Southern African Kalahari. *Remote Sensing Environ.*, 2002, **83**, 232–243.
8. Chen, J. M. and Cihlar, J., Retrieving leaf area index of boreal conifer forests using Landsat TM images. *Remote Sensing Environ.*, 1996, **55**, 153–162.
9. Myneni, R. B., Nemani, R. R. and Running, S. W., Estimation of global leaf area index and absorbed PAR using radiative transfer model. *IEEE Trans. Geosci. Remote Sensing*, 1997, **35**, 1380–1393.
10. Price, J. C., Estimating leaf area index from satellite data. *IEEE Trans. Geosci. Remote Sensing*, 1993, **31**, 727–734.
11. Gao, W. and Lesht, B. M., Model inversion of satellite-measured reflectances to obtain surface biophysical and bi-directional reflectance characteristics of grassland. *Remote Sensing Environ.*, 1997, **59**, 461–471.
12. Pandya, M. R., Singh, R. P., Murali, K. R., Babu, N., Kirankumar, A. S. and Dadhwal, V. K., Band pass solar exoatmospheric irradiance and Rayleigh optical thickness of sensors onboard Indian remote sensing satellites-1B, 1C, 1D and P4. *IEEE Trans. Geosci. Remote Sensing*, 2002, **40**, 714–718.
13. Vermote, E., Tanre, D., Deuze, J. L., Herman, M. and Morcrette, J. J., Second simulation of the satellite signal in the solar spectrum (6S), 6s User Guide version 2, 1997, p. 218.
14. Price, J. C., Estimating vegetation amount from red and near infrared reflectances. *Remote Sensing Environ.*, 1992, **41**, 29–34.
15. Rastogi, A., Kalra, N., Agarwal, P. K., Sharma, S. K., Harit, R. C., Navalgund, R. R. and Dadhwal, V. K., Estimation of wheat leaf area index from IRS LISS-III data using Price model. *Int. J. Remote Sensing*, 2000, **21**, 2943–2949.

Received 6 June 2003; accepted 28 August 2003

Molecular diagnosis and induced systemic protection against rhizome rot disease of ginger caused by *Pythium aphanidermatum*

R. Ghosh and R. P. Purkayastha*
Department of Botany, University of Calcutta, Kolkata 700 019, India

Polyclonal antibodies and antigens of host and pathogen were used for early diagnosis of rhizome rot disease of ginger. *Pythium aphanidermatum*, a causal organism was detected in ginger rhizome after eight weeks of inoculation by agar gel double diffusion and immuoelectrophoretic tests, but only one week after inoculation by indirect ELISA (enzyme linked immunosorbent assay). Systemic protection against *P. aphanidermatum* was induced in ginger (Cv. Suprabha) by soaking rhizome seeds separately in selected synthetic chemicals or specific herbal extracts for 1 h prior to sowing. Among 12 plant defence activators tested, jasmonic acid (JA, 5 mM) and 10% leaf extract of *Acalypha indica* (ALE) reduced disease significantly, with concomitant increase of defence-related proteins (DRPs). Analysis of protein profiles of leaves of JA-treated and inoculated plants by SDS–PAGE and Image Master VDS-ID Gel Analysis Version 3.0 revealed 18 protein bands, including four DRPs having molecular masses 32, 24, 18 and 14 kDa respectively. At least four DRPs were detected in leaves of ALE-treated inoculated plants. Growth response of pathogen to both JA and ALE was evaluated *in vitro*. ALE stimulated growth, while JA inhibited growth at high concentration (0.5 mM) and slightly stimulated growth at low dose (0.005 mM). Results suggest their host-mediated role in induced systemic protection against disease.

RHIZOME rot is a serious disease of ginger (*Zingiber officinale* Rosc.), causing considerable economic loss to growers in different countries. To ensure effective and sustainable disease management, early detection and authentic identification of pathogen are considered as prerequisites. On the contrary, exploitation of host defence is one of the most reliable non-conventional strategies of plant disease management. Several synthetic chemicals and natural products could induce or activate host resistance by producing or accumulating defence-related proteins (DRPs) or other antimicrobial compounds, as reported earlier by several workers[1–4]. Foliar spray with potassium phosphate (0.1 M) induced systemic protection against *Sphaerotheca fuliginea* (powdery mildew) in cucumber[5]. Similarly, potato leaves sprayed with jasmonic acid (JA) or jasmonate methyl ester (JME) also induced systemic protection against *Phytophthora infestans* and enhanced levels of two proteinase inhibitors[6]. In this communica-

*For correspondence. (e-mail: rajyasri_5@rediffmail.com)